Saudi Journal of Biological Sciences (2015) **22**, 42–49

King Saud University

Saudi Journal of Biological Sciences

www.ksu.edu.sa
www.sciencedirect.com

ORIGINAL ARTICLE

Improved efficiency and stability of secnidazole – An ideal delivery system

Salman Khan [a], Mohd Haseeb [a], Mohd Hassan Baig [a], Paramdeep Singh Bagga [b], H.H. Siddiqui [b], M.A. Kamal [c,d], Mohd Sajid Khan [a,*]

[a] *Department of Biosciences, Integral University, Lucknow 226026, Uttar Pradesh, India*
[b] *Faculty of Pharmacy, Integral University, Lucknow 226026, Uttar Pradesh, India*
[c] *King Fahd Medical Research Center, King Abdulaziz University, P.O. Box 80216, Jeddah 21589, Saudi Arabia*
[d] *Enzymoic, 7 Peterlee Pl, Hebersham, NSW 2770, Australia*

Received 17 February 2014; revised 24 May 2014; accepted 25 May 2014
Available online 13 June 2014

KEYWORDS

Nanoparticles;
Secnidazole;
Bioconjugation;
Drug delivery;
Biosynthesis

Abstract Secnidazole (α,2-Dimethyl-5-nitro-1H-imidazole-1-ethanol) is a highly effective drug against a variety of G^+/G^- bacteria but with significant side effects because it is being used in very high concentration. In this study, gold nanoparticles (GNP_S) were selected as a vehicle to deliver secnidazole drug at the specific site with more accuracy which made the drug highly effective at substantially low concentrations. The as-synthesized GNPs were capped with Human Serum Albumin (HSA) and subsequently bioconjugated with secnidazole because HSA provides the stability and improves the solubility of the bioconjugated drug, secnidazole. The quantification of covalently bioconjugated secnidazole with HSA encapsulated on enzymatically synthesized GNPs was done with RP-HPLC having SPD-20 A UV/VIS detector by using the C-18 column. The bioconjugation of GNPs with secnidazole was confirmed by Transmission Electron Microscopy (TEM) and Dynamic Light Scattering (DLS). The bioconjugated GNPs were characterized by UV–VIS spectroscopy, TEM, Scanning Electron Microscopy (SEM) and DLS. Zeta potential confirmed the stability and uniform distribution of particles in the emulsion of GNPs. The separation of bioconjugated GNPs, unused GNPs and unused drug was done by gel filtration chromatography. The minimal inhibitory concentration of secnidazole-conjugated gold nanoparticles (Au-HSA-Snd) against *Klebsiella pneumonia* (NCIM No. 2957) and *Bacillus cereus* (NCIM No. 2156) got improved by 12.2 times and 14.11 times, respectively, in comparison to pure secnidazole. Precisely, the MIC of Au-HSA-Snd against *K. pneumonia* (NCIM No. 2957) and *B. cereus* (NCIM No. 2156) were

* Corresponding author. Tel.: +91 522 2890812/2890730; fax: +91 522 2890809.
E-mail address: sajid_987@rediffmail.com (M.S. Khan).

Peer review under responsibility of King Saud University.

Production and hosting by Elsevier

1319-562X © 2014 Production and hosting by Elsevier B.V. on behalf of King Saud University.
http://dx.doi.org/10.1016/j.sjbs.2014.05.009

found to be 0.35 and 0.43 μg/ml, respectively whereas MIC of the pure secnidazole drug against the same bacteria were found to be 4.3 and 6.07 μg/ml, respectively.

© 2014 Production and hosting by Elsevier B.V. on behalf of King Saud University.

1. Introduction

Inorganic nanoparticles have emerged as one of the best drug delivery systems among the existing engineered nanomaterials (Mieszawska et al., 2014; Heo et al., 2012; Wu et al., 2005; Salem et al., 2003). They have wide bioavailability, low toxicity, rich functionality, and good biocompatibility, potential capability of targeted and controlled delivery. However, it is noted that the cellular transfer efficiency with existing inorganic nanoparticles is relatively low. Being chemically stable, inorganic nanoparticles remain unchanged during the whole delivery process and they should not be biodegraded in plasma and cytoplasm of a human body (Xu et al., 2006). Specifically, GNPs emerged as an attractive candidate for delivery of various biomolecules into their targets (Jin et al., 2014; Duncan et al., 2010; Pissuwan et al., 2011). GNPs can also be used as adjuvant for enhancing the efficacy of radiation therapy and as contrast agents for various modalities involved in therapeutic and diagnostic applications (Dorsey et al., 2013). GNPs have unique chemical and physical properties and can effectively transport and unload the pharmaceuticals in cellular systems. Moreover, photophysical properties of gold could trigger drug release at remote places (Skirtach et al., 2006; Connor et al., 2005). GNPs in particular are an excellent intracellular targeting vector because it can be engineered into desirable size, surface to achieve good biocompatibility with functionalities. GNPs have a widespread distribution in the human body, although internalization of GNPs depends upon the types of the cell (Coulter et al., 2012). The presence of GNPs could create an oxidative environment; it also affects the regulation of cellular stress response mechanisms and at the same time induces the formation of autophagosomes, possibly to protect the cell from succumbing to oxidative stress. Surface modification of GNPs also enhances the stability of biomolecules by improving zeta potential and reduces the side effects by preventing nonspecific interactions (He et al., 2003). It is interesting to mention that most modifiers provide a very good protection for biomolecules from being degraded by enzymes in plasma, which is largely due to the steric effect and electrostatic repulsion from the modifiers. Secnidazole (α,2-Dimethyl-5-nitro-1H-imidazole-1-ethanol) is structurally related to the commonly used 5-nitroimidazole metronidazole and tinidazole. The physicochemical, molecular and other related properties of the bulk drug have been established well (Wells, 1987). Nanoparticle mediated delivery systems have several distinguished advantages. In a normal drug administration, drug molecules affect the target cell as well as the nonspecific cells via blood circulation with no preference for drug molecules to recognize targeted cells. Whereas, in nanoparticle mediated drug delivery system surface fictionalization of the nanoparticles determines the driving forces for transfection (Zhu et al., 2004; Pinto-Alphandary et al., 2000; Tom et al., 2004). Also, grafting specific biomolecules on nanoparticles provides site specific delivery of nanoparticles into cells. Human Serum Albumin (HSA) is acidic in nature, soluble in a wide range of pH, has been used as a capping agent and linker between drug and nanoparticles. HSA, readily available, biodegradable, lacks toxicity and immunogenicity, makes the system more stable and efficient by protecting drugs by limiting nonspecific interactions markedly, which makes it an ideal system for drug delivery (Sripriyalakshmi et al., 2014). There are many reports, where nanocarriers have been proved to be a very effective cargo of the drugs like gentamycin (Lecaroz et al., 2006), ampicillin (Fattal et al., 1989), amphotericin B (Umamaheshwari et al., 2004), anticancer antibodies and drugs (Marega et al., 2012; Moghimi, 2006). Nanoconjugates also help in reducing the dose of certain drugs, as there are many drugs which are required in very high concentration in human body and hence produce toxic effect (Schellie and Groshong, 1999). The accurate effect of conjugated drug could be determined only if quantification of conjugated drug is exactly known. Hence, in the present study, an attempt was made to develop a two step method to biosynthesize HSA encapsulated gold nanoparticles and eventually, their bioconjugation with secnidazole. The secnidazole-conjugated gold nanoparticles (Au-HSA-Snd) were used against *Klebsiella pneumonia* (NCIM No. 2957) and *Bacillus cereus* (NCIM No. 2156). This system was found to be highly effective against these microbes in comparison to pure secnidazole.

2. Materials and methods

In this study *in vitro* synthesis of gold nanoparticles was done by taking a total reaction mixture of 3 ml containing 1.0 mM, each of freshly prepared $H[AuCl_4]$ and Na_2SO_3, 100 μg of Human Serum Albumin (HAS), 1.0 mM α-NADPH (α-Nicotinamide adenine dinucleotide phosphate, reduced disodium salt) and 1.66 U (100 μg protein) of sulfite reductase (Kumar et al., 2007). The reaction mixture was incubated, under anaerobic conditions at 25 °C. Reactions performed in the absence of α-NADPH enzyme, HSA and with the inactivated enzyme were used as a control. Samples were removed at regular intervals and analyzed in UV–VIS spectroscopy to confirm for the nanoparticle formation. On completion of the reaction, gold nanoparticles were collected by centrifugation (30,000*g*, 30 min), washed twice with Milli Q water and the unbound proteins were removed by treating with 50% v/v of 1,4-Dioxane and used for further characterization.

For characterization, UV–VIS spectrophotometry measurements were performed on a Shimadzu dual-beam spectrophotometer (model UV-1601 PC) operated at a resolution of 1 nm in the quartz cuvette.

Transmission Electron Microscopy (TEM) was done by drying a drop of gold nanoparticle solution on carbon coated TEM copper grids followed by measurements on (TEM) FEI Company, Tecnai™ G^2 Spirit BioTWIN operated at an accelerating voltage of 80 kV.

Scanning Electron Microscopy was done by drying a drop of as-synthesized GNP solution on glass slides and then coated

with gold. The morphology of nanoparticles was examined under a scanning electron microscope (JEOL JSM 5200).

The mean particle size of HSA encapsulated biosynthesized gold nanoparticles (Au-HSA) and secnidazole bioconjugated nanoparticles (Au-HSA-Snd) was measured with a Dynamic Light Scattering (DLS) particle size analyzer (Zetasizer Nano-ZS, Model ZEN3600, Malvern Instrument Ltd, Malvern, UK). The powder of the sample was diluted to a concentration of 0.5% (Wt/v) in deionized water and sonicated for 1 min before measurement. The sample was taken in a DTS0112-low volume disposable sizing cuvette of 1.5 ml. Mean particle size was the average of triplicate measurements for a single sample. Zeta potential was also measured using a Zetasizer Nano-ZS, Model ZEN3600 (Malvern Instrument Ltd, Malvern, UK).

In vitro synthesized Au-HSA nanoparticles were bioconjugated to secnidazole with the free carboxylate group present on HSA by using the activator 1-Ethyl-3-(3-dimethylaminopropyl)-carbodiimide (EDC) (Timkovich, 1977; Hermanson, 1996). The coupling was performed in a reaction mixture of 5 ml containing 50 mM MES/HEPES buffer, 250 μg of Secnidazole and 250 μg of Au-HSA nanoparticles whereas 5 mM EDC was added in aliquots within 3 hours at 30 °C in the reaction mixture.

Bioconjugates were separated from unconjugated Au-HSA nanoparticles by passing the reaction mixture through Biogel P-30 gel filtration column pre-equilibrated with 20 mM HEPES buffer (pH 6.0) containing 150 mM NaCl. The fractions were scanned between 200 and 900 nm and subsequently, those fractions were pooled which showed absorbance at 320 nm/525 nm due to the presence of secnidazole conjugated with Au-HSA nanoparticles. The pooled samples were dialyzed against distilled water and used for further characterization.

Further, Loading efficiency (LE) of secnidazole drug on Au-HSA nanoparticles was determined by a high performance liquid chromatography (A Shimadzu-model HPLC equipped LC-20 AT pump, SPD-20 A UV/VIS detector, Rheodyne injector fitted with a 20-μl loop was used and the data were recorded and evaluated using Spinchrom software) at 25 °C with a reversed-phase C-18 column, Luna Column (5 μm, 250 × 4.6 mm inner diameter) using a mobile phase consisting of buffer: 0.01 M KH_2PO_4: ACN (85:15) at a flow rate of 1 ml/min with UV detection at 228 nm. The mobile phase was filtered through 0.22-μm nylon filter prior to use. The experiments were performed in triplicate. Quantitative determination of secnidazole was performed according to the method described by Rivera et al. (2000). The pure drug calibration curve was plotted in the linear range of 2-25 μg/ml. The percentage loading of secnidazole to GNPs was calculated by using RP-HPLC C-18 column. The standard curve of the pure secnidazole drug was established and unbound drug was calculated from the standard curve. Amount of bioconjugated drug was calculated by subtracting unbound drug from the total amount of drug added. The exact amount of bioconjugated drug was calculated using the following equation:

$$\% \text{ Bioconjugation} = (\text{Amount of drug Bioconjugated} / \text{Total drug added}) \times 100$$

Efficacy of bioconjugated secnidazole was estimated by evaluating Minimum Inhibitory Concentration (MIC) of Au-HSA-Snd and pure secnidazole drug against *K. pneumonia* (NCIM No. 2957) and *B. cereus* (NCIM No. 2156) in Luria–Bertani (LB) broth using the protocol described by Amsterdam, 1991. Bacteria grown to mid-logarithmic phase were harvested by centrifugation, washed with 10 mM sodium phosphate buffer (SPB) at pH 7.4, and diluted to 2×10^5 colony forming units (CFU)/ml in SPB containing 0.03% Luria–Bertani (LB) broth. Au-HSA-Snd were serially diluted in 50 μL of LB medium in 96-well microtitre plates to achieve the desired concentrations with bacterial inoculum (5×10^4 CFU per well). After incubation at 37 °C overnight, the MIC was taken as the lowest Au-HSA-Snd concentration at which growth was inhibited. For the agar plate count method (Stenger et al., 1998), a 25 μL aliquot of bacteria at 1×10^5 CFU/ml in SPB containing 0.03% LB broth was incubated with 25 μL of diluted compounds for 2 h at 37 °C (Hamamoto et al., 2002). The mixtures were serially diluted 10-fold in SPB, plated on LB agar and incubated overnight at 37 °C. Bacterial colonies were enumerated the following day. Autoclaved water and only non conjugated gold nanoparticles (Au-HAS) were used as a negative control in the experiment. After having determined the MIC of bacteria from the wells of the microtitre plate with no visible bacterial growth, samples were removed for serial subcultivation of 2 μL into microtitre plates containing 100 μL of broth per well and further incubated for 24 h to determine the Bactericidal Activity Measurement (MBC). The lowest concentration with no visible growth was defined as MBC, indicating 99.5% killing of the original inoculums. The optical density of each well was measured at a wavelength of 620 nm by microtitre plate manager 4.0 (Bio-Rad laboratories) and compared with a control. Autoclaved water and only non conjugated gold nanoparticles (Au-HSA) were used as a negative control in the experiment. Two replicates were done for each compound and the experiment was repeated twice.

3. Results and discussion

The targeted delivery of drugs is one of the most promising and actively developing areas in the medicinal use of GNPs (Duncan et al., 2010). Antibiotics and antitumor agents are the most popular objects of target delivery. The conjugation of GNPs with a good number of drugs such as 6-mercaptopurine (Podsiadlo et al., 2008), 5-fluorouracil (Agasti et al., 2009), platinum complexes (Dhar et al., 2009), kahalalide (Hosta et al., 2009), doxorubicin (Asadishad et al., 2010), and many more has been done with great success. On the contrary, successful conjugations of antibiotics such as ampicillin, streptomycin, kanamycin, hentamycin, neomycin, ciprofloxacin, gatifloxacin, and norfloxacin were (Saha et al., 2007; Grace and Pandian, 2007) not done with gold nanoparticles. Nevertheless, they were found 12–40% more active when mixed with colloidal gold than that of the antibiotic used alone, depending on the antibiotic. Hence, it was proved that the antibacterial activity of antibiotics was enhanced by GNPs but stable conjugates of nanoparticles coated with antibiotic molecules are required to enhance the antibacterial activity exceptionally high. It has also been proved that upon intravenous injection, GNP conjugated with drugs rapidly accumulates in defected cells and is not detected in cells of the liver, spleen, and other healthy organs (Mukherjee et al., 2005). GNPs have antiangiogenic properties (Mukherjee et al., 2005) and enhance the

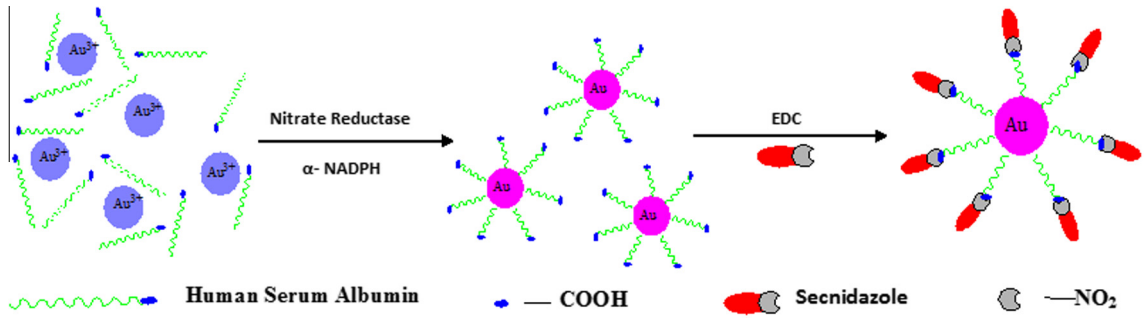

Figure 1 Schematic representation of biosynthesis of Human Serum Albumin capped Gold nanoparticles (Au-HSA) by using Nitrate Reductase as reducing agent and eventually their bioconjugation with secnidazole drug (Au-HSA-Snd).

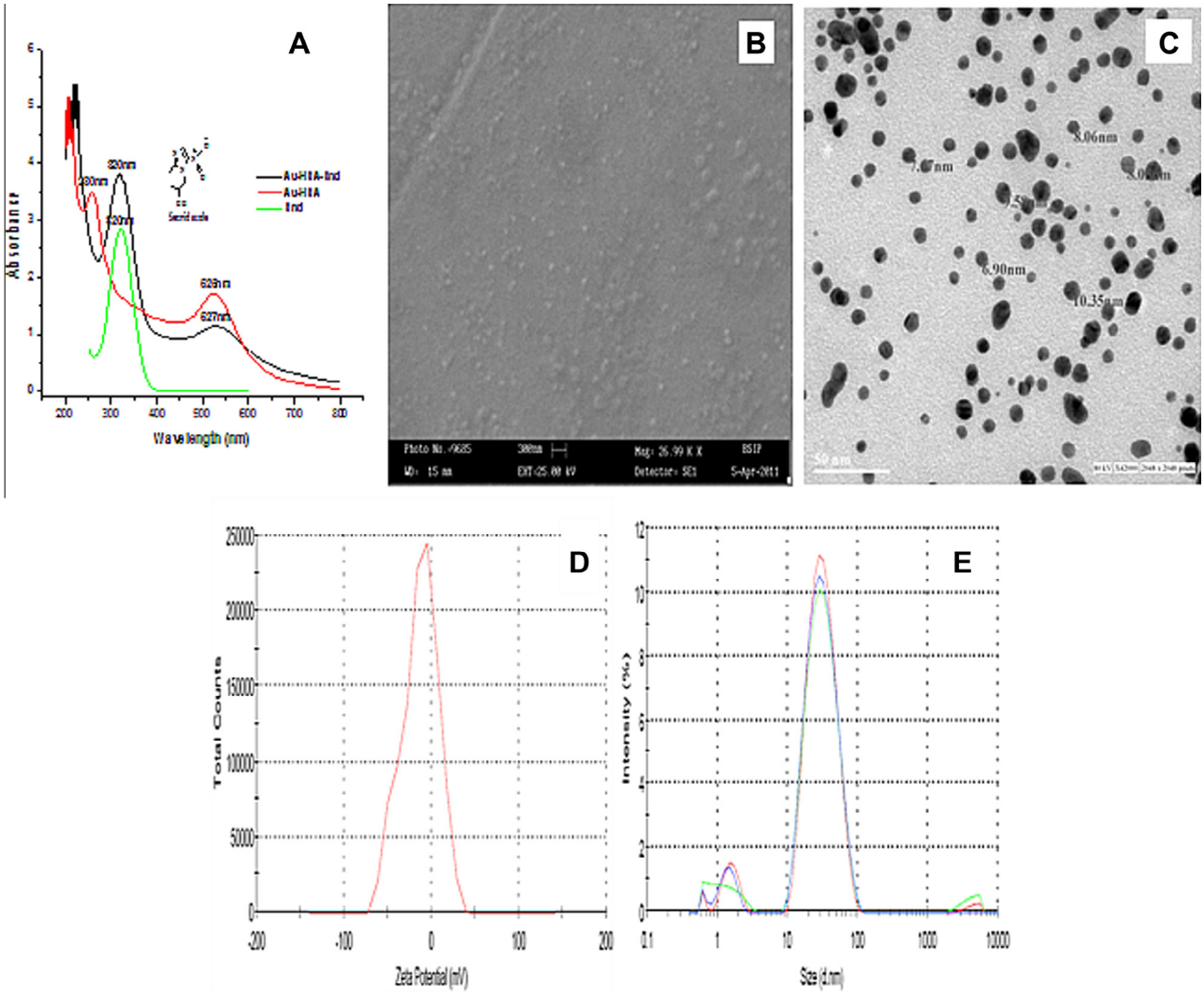

Figure 2 Characterization of HSA encapsulated bioengineered Pure GNP (GNP-HSA) under (A) UV–VIS spectroscopy (B) Scanning Electron Microscopy (B) Transmission Electron Microscopy (C) Zeta Potential and (D) Dynamic Light Scattering.

apoptosis of the cancer cells that are stable to programed death (Mukherjee et al., 2007) and suppress the proliferation of multiple myeloma cells (Bhattacharya et al., 2007).

There has been much less data on other drugs conjugated with gold nanoparticles (Dykman and Khlebtsov, 2011). In the present study, secnidazole was successfully bioconjugated with gold nanoparticles (Au-HSA) with accuracy and the effectiveness of gold nanoparticle bioconjugated secnidazole (Au-HSA-Snd) was tested against *K. pneumonia* (NCIM No. 2957) and *B. cereus* (NCIM No. 2156) in comparison to its unconjugated form. This system was used as a vehicle to deliver secnidazole effectively at the targeted cells. Fig. 1 illustrates

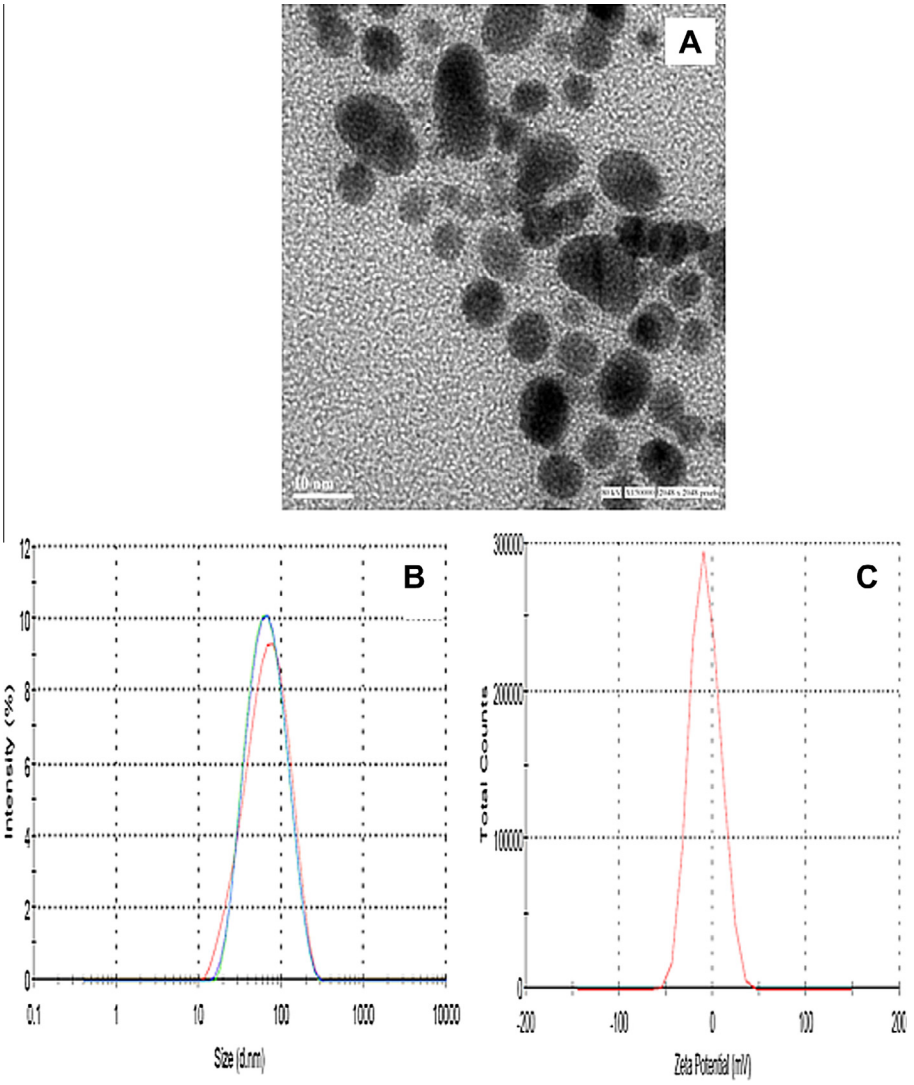

Figure 3 Characterization and confirmation of bioconjugation of secnidazole with Pure GNP (GNP-HSA) in order to synthesize secnidazole bioconjugated GNP (GNP-HSA-Snd) under (A) Transmission Electron Microscope (B) Dynamic Light Scattering and (C) Zeta Potential.

the schematic synthesis of Human Serum Albumin (HSA) encapsulated gold nanoparticles (Au-HSA) by nitrate reductase and eventually their bioconjugation with secnidazole drug. The formation of the Au-HSA has been confirmed by their representative surface plasmon resonance (SPR) band measured as measured by optical density in UV–VIS absorption spectroscopy. The SPR absorption spectra of Au-HSA and secnidazole-conjugated Human Serum Albumin coated gold nanoparticles (Au-HSA-Snd) are plotted in Fig. 2A. The size and concentration of GNPs between 5 and 100 nm can be determined by using the Classical Guass method (Wolfgang et al., 2007). The linear regression equation ($\lambda_{max} = 515.04 + 0.3647d$) explains the relation between particle diameter and λ_{max} (He et al., 2005). Hence, the absorbance band shifts toward red with the increase in diameter of the particles and intensity of peak decreases with a decrease in particle size due to the reduced mean free path of the electrons due to collisions of electrons with the particle surface (Haiss et al., 2007).

The topographical studies such as surface structure and morphology of Au-HSA, were performed under SEM and size of nanoparticles was determined manually using Gatan digital micrograph which showed spherical shaped nanoparticles with an average size of 7 ± 2 nm (Fig. 2B). High resolution images were acquired using TEM (Fig. 2C). The stability of the Au-HSA was confirmed by zeta potential which was found to be −13.3 mV (Fig 2D), which can be one of the reasons for their long term stability and the electrostatic repulsive forces between the nanoparticles might protect them from getting closer and thereby preventing agglomeration or clumping in aqueous suspension. Dynamic Light Scattering (DLS) also reveals that the particles are smaller in size and uniformly distributed (Fig 3E). The hydrodynamic diameter of nanoparticles appears large (18 ± 3 nm) in DLS due to the interaction and binding of solvent to the surface of nanoparticles. The bioconjugation of secnidazole with Au-HSA was confirmed by the SPR absorption band for Au-HSA-Snd which appeared at 525 nm, with a significant broadening and a slight decrease

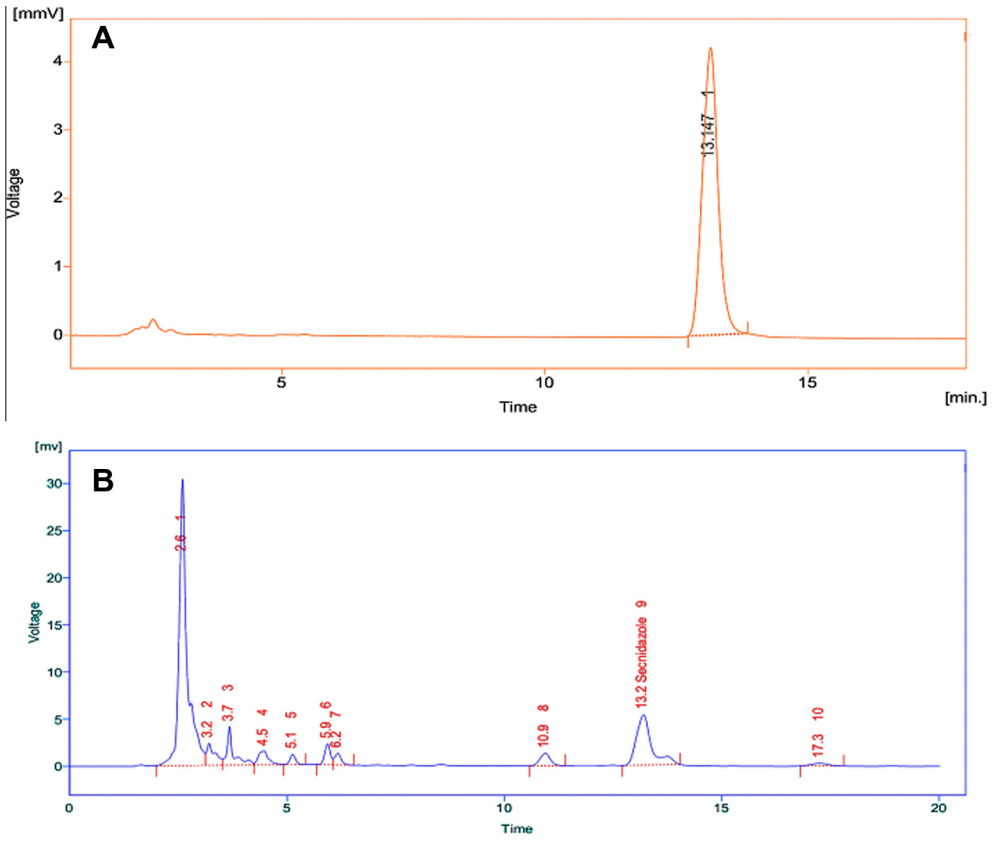

Figure 4 RP-HPLC chromatograms for (A) pure secnidazole drug and (B) bioconjugated drug (Au-HSA-Snd).

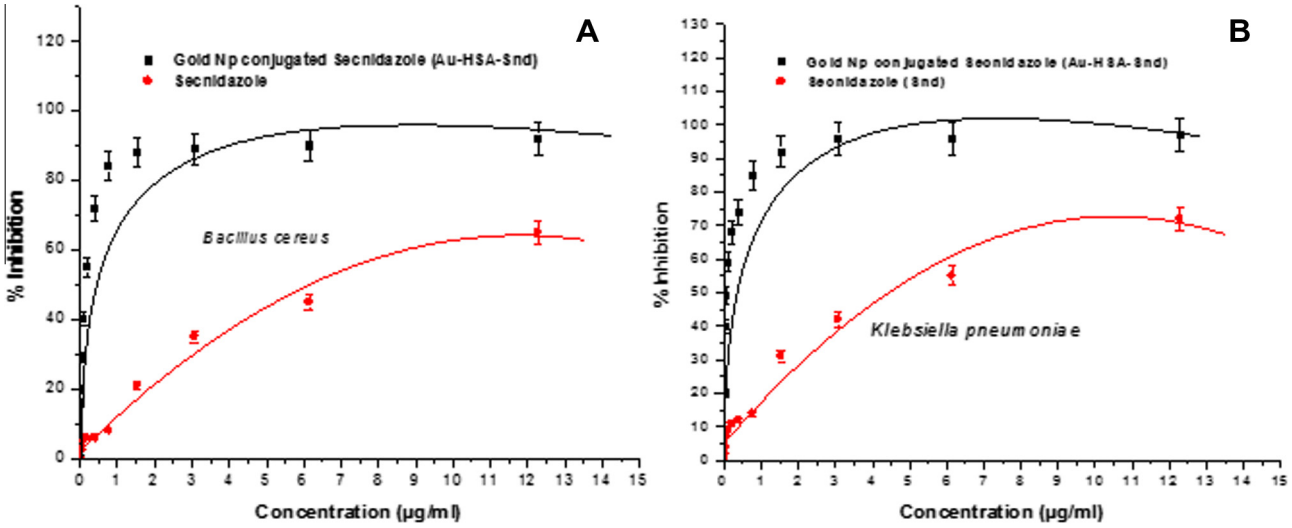

Figure 5 (A) Antibacterial test of secnidazole bioconjugated gold nanoparticles (GNP-HSA-Snd) in comparison to pure secnidazole drug against (A) *Bacillus cereus* (B) *Klebsiella pneumoniae*.

in intensity compared to the plasmon band for Au-HSA at 527 nm (Fig 2A) because the plasmon resonance is a surface phenomenon which alters after attachment of any ligand at the surface. The ligand binding significantly affects the absorption intensity and full width at half maximum (FWHM) of absorption band. The observed broadening in absorption band is attributed to the attachment of secnidazole drug at the surface of nanoparticles. The absorption spectrum of Au-HSA-Snd reveals two peaks at 320 nm and 525 nm are corresponding to secnidazole aromatic nitrite transitions and GNPs respectively, suggesting its binding to GNPs. Further, TEM micrographs of secnidazole-conjugated gold nanoparticles (Au-HSA-Snd) also reveal the attachment of secnidazole (and consequent enlargement of the particles) as a biomolecular layer at the surface, resulting in some blurring of the micrograph (3A). Also, secnidazole-conjugated gold

nanoparticles (Au-HSA-Snd) appear bigger than non conjugated (Au-HSA) one due to subsequent enlargement of nanoparticles (Fig 3B). The zeta potential of Au-HSA-Snd was found to be −7.97 mV which is well in the range required for stable emulsion (Fig 3C). The decrease in zeta potential may be attributed to the decrease of the free amino groups on the Au-HSA-Snd after bioconjugation of the secnidazole drug to these groups. The quantitative estimation of bioconjugated secnidazole with Au-HSA was determined by RP-HPLC chromatography by using the C-18 column. The amount of bioconjugated secnidazole was found to be 70% indicating efficient binding of secnidazole with Au-HSA-Snd nanoparticles (Fig 4). The retention time for pure secnidazole drug and Au-HSA-Snd is 13.147 min (Fig 4A) and 13.2 min (Fig 4B), respectively. The slight change in retention time is due to variation of pH in the mobile phase to the medium of drug. The retention time for gold nanoparticle bound secnidazole is 2.6 min (Fig 4B). Au-HSA-Snd Au-HSA-Snd nanoparticles and pure secnidazole drug (Fig 5) were evaluated for antibacterial activity against representative bacteria *K. pneumonia* (NCIM No. 2957) and *B. cereus* (NCIM No. 2156). Autoclaved water and only Au-HSA were used as negative control. The MIC of Au-HSA-Snd nanoparticles against *K. pneumonia* (NCIM No. 2957) and *B. cereus* (NCIM No. 2156) were found to be 0.35 μg/ml and 0.43 μg/ml, respectively, whereas MIC of the pure secnidazole drug against *K. pneumonia* (NCIM No. 2957) and *B. cereus* (NCIM No. 2156) were found to be 4.3 and 6.07 μg/ml, respectively. The efficiency of bioconjugated secnidazole got improved by 12.2 and 14.11 times, respectively, in comparison to pure secnidazole. The pure gold nanoparticles were not found to be toxic against any bacterial strain. In conclusion, Secnidazole-bioconjugated Human Serum Albumin coated gold nanoparticles (Au-HSA-Snd) were developed as a suitable vehicle for targeting drug delivery system to enhance therapeutic effects of secnidazole drug and reduce its side effects. Although there are certain limitations of this system that all drugs cannot be bioconjugated with gold nanoparticles and their toxicity level changes with change in drug. In future a detailed mechanism of action including internalization in the targeted cells of Au-HSA-Snd has to be elucidated to make drug even more effective.

4. Conclusions

Secnidazole-bioconjugated Human Serum Albumin coated gold nanoparticles (Au-HSA-Snd) were developed as an ideal targeted drug delivery system to enhance therapeutic effects significantly of secnidazole drug and reduce its side effects. This system not only makes the drug stable, but also reduces the dose with enhanced potency.

Acknowledgements

We thank the Uttar Pradesh Council of Science and Technology (UPCST), Government of India, for financial assistance. This work was supported by a grant to Dr. Mohd Sajid Khan from UPCST, India.

References

Agasti, S.S., Chompoosor, A., You, C.C., Ghosh, P., Kim, C.K., Rotello, V.M., 2009. Photoregulated release of caged anticancer drugs from gold nanoparticles. J. Am. Chem. Soc. 131, 5728–5729.

Amsterdam, D., 1991. Susceptibility testing of antimicrobials in liquid media. In: V. Lorian (Ed.), Antibiotics in Laboratory Medicine. Baltimore, Williams & Wilkinsp, pp. 172–178.

Asadishad, B., Vossoughi, M., Alemzadeh, I., 2010. Folate-receptor-targeted delivery of doxorubicin using polyethylene glycol-functionalized gold nanoparticles. Ind. Eng. Chem. Res. 49, 1958–1963.

Bhattacharya, R., Patra, C.R., Verma, R., Kumar, S., Greipp, P.R., Mukherjee, P., 2007. Gold nanoparticles inhibit the proliferation of multiple myeloma cells. Adv. Mater. 19, 711–716.

Connor, E.E., Mwamuka, J., Gole, A., Murphy, C.J., Wyatt, M.D., 2005. Gold nanoparticles are taken up by human cells but do not cause acute cytotoxicity. Small 1, 325–327.

Coulter, J.A., Jain, S., Butterworth, K.T., Taggart, L.E., Dickson, G.R., McMahon, S.J., Hyland, W.B., Muir, M.F., Trainor, C., Hounsell, A.R., O'Sullivan, J.M., Schettino, G., Currell, F.J., Hirst, D.G., Prise, K.M., 2012. Cell type-dependent uptake, localization, and cytotoxicity of 1.9 nm gold nanoparticles. Int. J. Nanomed. 7, 2673–2685.

Dhar, S., Daniel, W.L., Giljohann, D.A., Mirkin, C.A., Lippard, S.J., 2009. Polyvalent oligonucleotide gold nanoparticle conjugates as delivery vehicles for platinum(IV) warheads. J. Am. Chem. Soc. 131, 14652–14653.

Dorsey, J.F., Sun, L., Joh, D.Y., Witztum, A., Zaki, A.A., Kao, G.D., Basanta, M.A., Avery, S., Tsourkas, A., Hahn, S.M., 2013. Gold nanoparticles in radiation research: potential applications for imaging and radiosensitization. Transl. Cancer Res. 2, 280-29.

Duncan, B., Kim, C., Rotello, V.M., 2010. Gold nanoparticle platforms as drug and biomacromolecule delivery systems. J. Control. Release 148, 122–127.

Dykman, L.A., Khlebtsov, N.G., 2011. Gold nanoparticles in biology and medicine: recent advances and prospects. Acta Nat. 2, 34–55.

Fattal, E., Youssef, M., Couvreur, P., Andremont, A., 1989. Treatment of experimental salmonellosis in mice with ampicillin-bound nanoparticles. Antimicrob. Agents Chemother. 33, 1540–1543.

Grace, A.N., Pandian, K., 2007. Organically dispersible gold and platinum nanoparticles using aromatic amines as phase transfer and reducing agent and their applications in electro-oxidation of glucose. Colloids Surf. A 297, 63–70.

Haiss, W., Thanh, N.T.K., Aveyard, J., Fernig, D.G., 2007. Determination of size and concentration of gold nanoparticles from UV−VIS spectra. Anal. Chem. 79, 4215–4221.

Hamamoto, K., Kida, Y., Zhang, Y., Shimizu, T., Kuwano, K., 2002. Antimicrobial activity and stability to proteolysis of small linear cationic peptides with d-amino acid substitutions. Microbiol. Immunol. 46, 741–749.

He, X., Wang, K., Li, D., Tan, W., He, C., Huang, S., Liu, B., Lin, A., Chen, X.A., 2003. Novel DNA-enrichment technology based on aminomodified functionalised silica nanoparticles. J. Disp. Sci. Technol. 24, 633–640.

He, Y.Q., Liu, S.P., Kong, L., Liu, Z.F., 2005. A study on the sizes and concentrations of gold nanoparticles by spectra of absorption, resonance Rayleigh scattering and resonance non-linear scattering. Spectrochim. Acta 61, 2861–2866.

Heo, D.N., Yang, D.H., Moon, H.J., Lee, J.B., Bae, M.S., Lee, S.C., Lee, W.J., Sun, I.C., Kwon, I.K., 2012. Gold nanoparticles surface-functionalized with paclitaxel drug and biotin receptor as theranostic agents for cancer therapy. Biomaterials 33, 856–866.

Hermanson, G.T., 1996. The Definitive Source for Information on Protein Crosslinking, Labeling and Surface Attachment. Bioconjugate Techniques. Academic Press.

Hosta, L., Pla-Roca, M., Arbiol, J., López-Iglesias, C., Samitier, J., Cruz, L.J., Kogan, M.J., Albericio, F., 2009. Conjugation of Kahalalide F with gold nanoparticles to enhance in vitro antitumoral activity. Bioconjug. Chem. 20, 138–146.

Jin, S.E., Jin, H.E., Hong, S.S., 2014. Targeted delivery system of nanobiomaterials in anticancer therapy: from cells to clinics. Biomed. Res. Int. 2014, 814208.

Kumar, S.A., Abyaneh, M.K., Gosavi, S.W., Kulkarni, S.K., Ahmad, A., Khan, M.I., 2007. Sulfite reductase-mediated synthesis of gold nanoparticles capped with phytochelatin. Biotech. Appl. Biochem. 47, 191–195.

Lecaroz, C., Gamazo, C., Blanco-Prieto, M.J., 2006. Nanocarriers with gentamicin to treat intracellular pathogens. J. Nanosci. Nanotechnol. 6, 3296–3302.

Marega, R., Karmani, L., Flamant, L., Nageswaran, P.G., Valembois, V., Masereel, B., Feron, O., Borght, T.V., Lucas, S., Michiels, C., Gallez, B., Bonifazi, D., 2012. Antibody-functionalized polymer-coated gold nanoparticles targeting cancer cells: an in vitro and in vivo study. J. Mater. Chem. 22, 21305–21312.

Mieszawska, A.J., Mulder, W.J.M., Fayad, Z.A., Cormode, D.P., 2014. Multifunctional gold nanoparticles for diagnosis and therapy of disease. Mol. Pharm. 10, 831–847.

Moghimi, S.M., 2006. Recent developments in polymeric nanoparticle engineering and their applications in experimental and clinical oncology. Anticancer Agents Med. Chem. 6, 553–561.

Mukherjee, P., Bhattacharya, R., Wang, P., Wang, L., Basu, S., Nagy, J.A., Atala, A., Mukhopadhyay, D., Soker, S., 2005. Clin. Cancer Res. 11, 3530–3534.

Mukherjee, P., Bhattacharya, R., Bone, N., Lee, Y.K., Patra, C.R., Wang, S., Lu, L., Secreto, C., Banerjee, P.C., Yaszemski M.J., Kay, N.E., Mukhopadhyay, D., 2007. J. Nanobiotechnol. 5. <http://www.jnanobiotechnology.com/con-tent/5/1/4>.

Pinto-Alphandary, H., Andremont, A., Couvreur, P., 2000. Targeted delivery of antibiotics using liposomes and nanoparticles. Int. J. Antimicrob. Agents 13, 155–168.

Pissuwan, D., Niidome, T., Cortie, M.B., 2011. The forthcoming applications of gold nanoparticles in drug and gene delivery systems. J. Control. Release 149, 65–71.

Podsiadlo, P., Sinani, V.A., Bahng, J.H., Kam, N.W., Lee, J., Kotov, N.A., 2008. Gold nanoparticles enhance the anti-leukemia action of a 6-mercaptopurine chemotherapeutic agent. Langmuir 24, 568–574.

Rivera, A.B., Hernandez, R.G., Armas, H.N., Elizastegi, D.M.C., Losada, M.V., 2000. Physicochemical and solid-state characterization of secnidazole. IL Farmaco 55, 700–707.

Saha, B., Bhattacharya, J., Mukherjee, A., Ghosh, A.K., Santra, C.R., Dasgupta, A.K., Karmakar, P., 2007. Nanoscale Res. Lett. 2, 614–622.

Salem, A.K., Searson, P.C., Leong, K.W., 2003. Multifunctional nanorods for gene delivery. Nat. Mater. 2, 668–671.

Schellie, S.F., Groshong, T., 1999. Acute interstitial nephritis following amoxicillin overdose. Mol. Med. 96, 209–211.

Skirtach, A.G., Javier, A.M., Kreft, O., Kohler, K., Alberola, A.P., Mohwald, H., Parak, W.J., Sukhorukov, G.B., 2006. Laser-induced release of encapsulated materials inside living cells. Angew. Chem. Int. Ed. 45, 4612–4617.

Sripriyalakshmi, S., Anjali, C.H., George Priya Doss, C. Rajith, B., Ravindran, A., 2014. BSA nanoparticle loaded atorvastatin calcium – a new facet for an old drug. PLoS One 9, e86317.

Stenger, S., Hanson, D.A., Teitelbaum, R., Dewan, P., Niazi, K.R., Froelich, C.J., et al, 1998. An antimicrobial activity of cytolytic T cells mediated by granulysin. Science 282, 121–125.

Timkovich, R., 1977. Detection of the stable addition of carbodiimide to proteins. Anal. Biochem. 20, 138–143.

Tom, R.T., Suryanarayanan, V., Reddy, P.G., Baskaran, S., Pradeep, T., 2004. Ciprofloxacin-protected gold nanoparticles. Langmuir 20, 1909–1914.

Umamaheshwari, R.B., Ramteke, S., Jain, N.K., 2004. Anti-helicobacter pylori effect of mucoadhesive nanoparticles bearing amoxicillin in experimental gerbils model. AAPS Pharm. Sci. Technol. 5 (2), e32.

Wells, J.I., 1987. Pharmaceutical Preformulation: The Physicochemical Properties of Drug Substances. Wiley.

Wolfgang, H., Nguyen, T.K.T., Jenny, A., David, G.F., 2007. Determination of size and concentration of gold nanoparticles from UV–Vis spectra. Anal. Chem. 79, 4215–4221.

Wu, W., Wieckowski, S., Pastorin, G., Benincasa, M., Klumpp, C., Briand, J.P., Gennaro, R., Prato, M., Bianco, A., 2005. Targeted delivery of amphotericin B to cells by using functionalized carbon nanotubes. Angew. Chem. Int. Ed. 44, 6358–6362.

Xu, Z.P., Zeng, Q.H., Lu, G.Q., Yu, A.B., 2006. Inorganic nanoparticles as carriers for efficient cellular delivery. Chem. Eng. Sci. 61, 1027–1040.

Zhu, S.G., Xiang, J.J., Li, X.L., Shen, S.R., Lu, H.B., Zhou, J., Xiong, W., Zhang, B.C., Nie, X.M., Zhou, M., Tang, K., Li, G.Y., 2004. Poly(1-lysine)-modified silica nanoparticles for the delivery of antisense oligonucleotides. Biotechnol. Appl. Biochem. 39, 179–187.